

Search for scalar leptoquark pairs decaying to $\nu\bar{\nu}q\bar{q}$ in $p\bar{p}$ collisions at $\sqrt{s} = 1.96$ TeV

D. Acosta,¹⁶ J. Adelman,¹² T. Affolder,⁹ T. Akimoto,⁵⁴ M. G. Albrow,¹⁵ D. Ambrose,¹⁵ S. Amerio,⁴² D. Amidei,³³ A. Anastassov,⁵⁰ K. Anikeev,¹⁵ A. Annovi,⁴⁴ J. Antos,¹ M. Aoki,⁵⁴ G. Apollinari,¹⁵ T. Arisawa,⁵⁶ J-F. Arguin,³² A. Artikov,¹³ W. Ashmanskas,¹⁵ A. Attal,⁷ F. Azfar,⁴¹ P. Azzi-Bacchetta,⁴² N. Bacchetta,⁴² H. Bachacou,²⁸ W. Badgett,¹⁵ A. Barbaro-Galtieri,²⁸ G. J. Barker,²⁵ V. E. Barnes,⁴⁶ B. A. Barnett,²⁴ S. Baroiant,⁶ G. Bauer,³¹ F. Bedeschi,⁴⁴ S. Behari,²⁴ S. Belforte,⁵³ G. Bellettini,⁴⁴ J. Bellinger,⁵⁸ A. Belloni,³¹ E. Ben-Haim,¹⁵ D. Benjamin,¹⁴ A. Beretvas,¹⁵ A. Bhatti,⁴⁸ M. Binkley,¹⁵ D. Bisello,⁴² M. Bishai,¹⁵ R. E. Blair,² C. Blocker,⁵ K. Bloom,³³ B. Blumenfeld,²⁴ A. Bocci,⁴⁸ A. Bodek,⁴⁷ G. Bolla,⁴⁶ A. Bolshov,³¹ D. Bortoletto,⁴⁶ J. Boudreau,⁴⁵ S. Bourov,¹⁵ C. Bromberg,³⁴ E. Brubaker,¹² J. Budagov,¹³ H. S. Budd,⁴⁷ K. Burkett,¹⁵ G. Busetto,⁴² P. Bussey,¹⁹ K. L. Byrum,² S. Cabrera,¹⁴ M. Campanelli,¹⁸ M. Campbell,³³ F. Canelli,⁷ A. Canepa,⁴⁶ M. Casarsa,⁵³ D. Carlsmith,⁵⁸ S. Carron,¹⁴ R. Carosi,⁴⁴ M. Cavalli-Sforza,³ A. Castro,⁴ P. Catastini,⁴⁴ D. Cauz,⁵³ A. Cerri,²⁸ L. Cerrito,²³ J. Chapman,³³ Y. C. Chen,¹ M. Chertok,⁶ G. Chiarelli,⁴⁴ G. Chlachidze,¹³ F. Chlebana,¹⁵ I. Cho,²⁷ K. Cho,²⁷ D. Chokheli,¹³ J. P. Chou,²⁰ S. Chuang,⁵⁸ K. Chung,¹¹ W-H. Chung,⁵⁸ Y. S. Chung,⁴⁷ M. Cijliak,⁴⁴ C. I. Ciobanu,²³ M. A. Ciocci,⁴⁴ A. G. Clark,¹⁸ D. Clark,⁵ M. Coca,¹⁴ A. Connolly,²⁸ M. Convery,⁴⁸ J. Conway,⁶ B. Cooper,³⁰ K. Copic,³³ M. Cordelli,¹⁷ G. Cortiana,⁴² J. Cranshaw,⁵² A. Cruz,¹⁶ J. Cuevas,¹⁰ R. Culbertson,¹⁵ C. Currat,²⁸ D. Cyr,⁵⁸ D. Dagenhart,⁵ S. Da Ronco,⁴² S. D'Auria,¹⁹ P. de Barbaro,⁴⁷ S. De Cecco,⁴⁹ G. De Lentdecker,⁴⁷ M. Dell'Orso,⁴⁴ A. Deisher,²⁸ S. Demers,⁴⁷ L. Demortier,⁴⁸ M. Deninno,⁴ D. De Pedis,⁴⁹ P. F. Derwent,¹⁵ C. Dionisi,⁴⁹ J. R. Dittmann,¹⁵ P. DiTuro,⁵⁰ C. Doerr,²⁵ A. Dominguez,²⁸ S. Donati,⁴⁴ M. Donega,¹⁸ J. Donini,⁴² M. D'Onofrio,¹⁸ T. Dorigo,⁴² K. Ebina,⁵⁶ J. Efron,³⁸ J. Ehlers,¹⁸ R. Ely,²⁸ R. Erbacher,⁶ M. Erdmann,²⁵ D. Errede,²³ S. Errede,²³ R. Eusebi,⁴⁷ H-C. Fang,²⁸ S. Farrington,²⁹ I. Fedorko,⁴⁴ W. T. Fedorko,¹² R. G. Feild,⁵⁹ M. Feindt,²⁵ J. P. Fernandez,⁴⁶ R. D. Field,¹⁶ G. Flanagan,³⁴ L. R. Flores-Castillo,⁴⁵ A. Foland,²⁰ S. Forrester,⁶ G. W. Foster,¹⁵ M. Franklin,²⁰ J. C. Freeman,²⁸ Y. Fujii,²⁶ I. Furic,¹² A. Gajjar,²⁹ J. Galyardt,¹¹ M. Gallinaro,⁴⁸ M. Garcia-Sciveres,²⁸ A. F. Garfinkel,⁴⁶ C. Gay,⁵⁹ H. Gerberich,¹⁴ D. W. Gerdes,³³ E. Gerchtein,¹¹ S. Giagu,⁴⁹ P. Giannetti,⁴⁴ A. Gibson,²⁸ K. Gibson,¹¹ C. Ginsburg,¹⁵ K. Giolo,⁴⁶ M. Giordani,⁵³ M. Giunta,⁴⁴ G. Giurgiu,¹¹ V. Glagolev,¹³ D. Glenzinski,¹⁵ M. Gold,³⁶ N. Goldschmidt,³³ D. Goldstein,⁷ J. Goldstein,⁴¹ G. Gomez,¹⁰ G. Gomez-Ceballos,³¹ M. Goncharov,⁵¹ O. González,⁴⁶ I. Gorelov,³⁶ A. T. Goshaw,¹⁴ Y. Gotra,⁴⁵ K. Goulianos,⁴⁸ A. Gresele,⁴ M. Griffiths,²⁹ C. Grosso-Pilcher,¹² U. Grundler,²³ J. Guimaraes da Costa,²⁰ C. Haber,²⁸ K. Hahn,⁴³ S. R. Hahn,¹⁵ E. Halkiadakis,⁴⁷ A. Hamilton,³² B-Y. Han,⁴⁷ R. Handler,⁵⁸ F. Happacher,¹⁷ K. Hara,⁵⁴ M. Hare,⁵⁵ R. F. Harr,⁵⁷ R. M. Harris,¹⁵ F. Hartmann,²⁵ K. Hatakeyama,⁴⁸ J. Hauser,⁷ C. Hays,¹⁴ H. Hayward,²⁹ B. Heinemann,²⁹ J. Heinrich,⁴³ M. Hennecke,²⁵ M. Herndon,²⁴ C. Hill,⁹ D. Hirschbuehl,²⁵ A. Hocker,⁴⁷ K. D. Hoffman,¹² A. Holloway,²⁰ S. Hou,¹ M. A. Houlden,²⁹ B. T. Huffman,⁴¹ Y. Huang,¹⁴ R. E. Hughes,³⁸ J. Huston,³⁴ K. Ikado,⁵⁶ J. Incandela,⁹ G. Introzzi,⁴⁴ M. Iori,⁴⁹ Y. Ishizawa,⁵⁴ C. Issever,⁹ A. Ivanov,⁴⁷ Y. Iwata,²² B. Iyutin,³¹ E. James,¹⁵ D. Jang,⁵⁰ B. Jayatilaka,³³ D. Jeans,⁴⁹ H. Jensen,¹⁵ E. J. Jeon,²⁷ M. Jones,⁴⁶ K. K. Joo,²⁷ S. Jun,¹¹ T. Junk,²³ T. Kamon,⁵¹ J. Kang,³³ M. Karagoz Unel,³⁷ P. E. Karchin,⁵⁷ S. Kartal,¹⁵ Y. Kato,⁴⁰ Y. Kemp,²⁵ R. Kephart,¹⁵ U. Kerzel,²⁵ V. Khotilovich,⁵¹ B. Kilminster,³⁸ D. H. Kim,²⁷ H. S. Kim,²³ J. E. Kim,²⁷ M. J. Kim,¹¹ M. S. Kim,²⁷ S. B. Kim,²⁷ S. H. Kim,⁵⁴ Y. K. Kim,¹² M. Kirby,¹⁴ L. Kirsch,⁵ S. Klimentenko,¹⁶ M. Klute,³¹ B. Knuteson,³¹ B. R. Ko,¹⁴ H. Kobayashi,⁵⁴ D. J. Kong,²⁷ K. Kondo,⁵⁶ J. Konigsberg,¹⁶ K. Kordas,³² A. Korn,³¹ A. Korytov,¹⁶ A. V. Kotwal,¹⁴ A. Kovalev,⁴³ J. Kraus,²³ I. Kravchenko,³¹ A. Kreymer,¹⁵ J. Kroll,⁴³ M. Kruse,¹⁴ V. Krutelyov,⁵¹ S. E. Kuhlmann,² S. Kwang,¹² A. T. Laasanen,⁴⁶ S. Lai,³² S. Lami,⁴⁸ S. Lammel,¹⁵ M. Lancaster,³⁰ R. Lander,⁶ K. Lannon,³⁸ A. Lath,⁵⁰ G. Latino,³⁶ I. Lazzizzera,⁴² C. Lecci,²⁵ T. LeCompte,² J. Lee,²⁷ J. Lee,⁴⁷ S. W. Lee,⁵¹ R. Lefèvre,³ N. Leonardo,³¹ S. Leone,⁴⁴ S. Levy,¹² J. D. Lewis,¹⁵ K. Li,⁵⁹ C. Lin,⁵⁹ C. S. Lin,¹⁵ M. Lindgren,¹⁵ E. Lipeles,⁸ T. M. Liss,²³ A. Lister,¹⁸ D. O. Litvintsev,¹⁵ T. Liu,¹⁵ Y. Liu,¹⁸ N. S. Lockyer,⁴³ A. Loginov,³⁵ M. Loretì,⁴² P. Loverre,⁴⁹ R-S. Lu,¹ D. Lucchesi,⁴² P. Lujan,²⁸ P. Lukens,¹⁵ G. Lungu,¹⁶ L. Lyons,⁴¹ J. Lys,²⁸ R. Lysak,¹ E. Lytken,⁴⁶ D. MacQueen,³² R. Madrak,²⁰ K. Maeshima,¹⁵ P. Maksimovic,²⁴ G. Manca,²⁹ R. Marginean,³⁸ F. Margaroli,⁴ C. Marino,²³ M. Martin,²⁴ A. Martin,⁵⁹ V. Martin,³⁷ M. Martínez,³ T. Maruyama,⁵⁴ H. Matsunaga,⁵⁴ M. Mattson,⁵⁷ P. Mazzanti,⁴ K. S. McFarland,⁴⁷ D. McGivern,³⁰ P. M. McIntyre,⁵¹ P. McNamara,⁵⁰ R. McNulty,²⁹ A. Mehta,²⁹ A. Menzione,⁴⁴ P. Merkel,¹⁵ C. Mesropian,⁴⁸ A. Messina,⁴⁹ T. Miao,¹⁵ N. Miladinovic,⁵ J. Miles,³¹ L. Miller,²⁰ R. Miller,³⁴ J. S. Miller,³³ C. Mills,⁹ R. Miquel,²⁸ S. Miscetti,¹⁷ G. Mitselmakher,¹⁶ A. Miyamoto,²⁶ N. Moggi,⁴ B. Mohr,⁷ R. Moore,¹⁵ M. Morello,⁴⁴ P. A. Movilla Fernandez,²⁸ J. Muelmenstaedt,²⁸ A. Mukherjee,¹⁵ M. Mulhearn,³¹ T. Muller,²⁵ R. Mumford,²⁴ A. Munar,⁴³ P. Murat,¹⁵ J. Nachtman,¹⁵ S. Nahn,⁵⁹ I. Nakamura,⁴³ A. Napier,⁵⁵ R. Naporá,²⁴ D. Naumov,³⁶ V. Necula,¹⁶ J. Nielsen,²⁸ T. Nelson,¹⁵ C. Neu,⁴³ M. S. Neubauer,⁸ T. Nigmanov,⁴⁵ L. Nodulman,² O. Norriella,³ T. Ogawa,⁵⁶ S. H. Oh,¹⁴ Y. D. Oh,²⁷ T. Ohsugi,²² T. Okusawa,⁴⁰ R. Oldeman,⁴⁹ R. Orava,²¹ W. Orejudos,²⁸ K. Osterberg,²¹ C. Pagliarone,⁴⁴ E. Palencia,¹⁰ R. Paoletti,⁴⁴ V. Papadimitriou,¹⁵ A. A. Paramonov,¹²

S. Pashapour,³² J. Patrick,¹⁵ G. Pauletta,⁵³ M. Paulini,¹¹ C. Paus,³¹ D. Pellett,⁶ A. Penzo,⁵³ T. J. Phillips,¹⁴ G. Piacentino,⁴⁴ J. Piedra,¹⁰ K. T. Pitts,²³ C. Plager,⁷ L. Pondrom,⁵⁸ G. Pope,⁴⁵ X. Portell,³ O. Poukhov,¹³ N. Pounder,⁴¹ F. Prakashy, ¹³ A. Pronko,¹⁶ J. Proudfoot,² F. Ptohos,¹⁷ G. Punzi,⁴⁴ J. Rademacker,⁴¹ A. Rahaman,⁴⁵ A. Rakitine,³¹ S. Rappoccio,²⁰ F. Ratnikov,⁵⁰ H. Ray,³³ B. Reiser,¹⁵ V. Rekovic,³⁶ P. Renton,⁴¹ M. Rescigno,⁴⁹ F. Rimondi,⁴ K. Rinnert,²⁵ L. Ristori,⁴⁴ W. J. Robertson,¹⁴ A. Robson,⁴¹ T. Rodrigo,¹⁰ S. Rolli,⁵⁵ R. Roser,¹⁵ R. Rossin,⁴² C. Rott,⁴⁶ J. Russ,¹¹ V. Rusu,¹² A. Ruiz,¹⁰ D. Ryan,⁵⁵ H. Saarikko,²¹ S. Sabik,³² A. Safonov,⁶ R. St. Denis,¹⁹ W. K. Sakumoto,⁴⁷ G. Salamanna,⁴⁹ D. Saltzberg,⁷ C. Sanchez,³ L. Santi,⁵³ S. Sarkar,⁴⁹ K. Sato,⁵⁴ P. Savard,³² A. Savoy-Navarro,¹⁵ P. Schlabach,¹⁵ E. E. Schmidt,¹⁵ M. P. Schmidt,⁵⁹ M. Schmitt,³⁷ T. Schwarz,³³ L. Scodellaro,¹⁰ A. L. Scott,⁹ A. Scribano,⁴⁴ F. Scuri,⁴⁴ A. Sedov,⁴⁶ S. Seidel,³⁶ Y. Seiya,⁴⁰ A. Semenov,¹³ F. Semeria,⁴ L. Sexton-Kennedy,¹⁵ I. Sfiligoi,¹⁷ M. D. Shapiro,²⁸ T. Shears,²⁹ P. F. Shepard,⁴⁵ D. Sherman,²⁰ M. Shimojima,⁵⁴ M. Shochet,¹² Y. Shon,⁵⁸ I. Shreyber,³⁵ A. Sidoti,⁴⁴ M. Siket,¹ A. Sill,⁵² P. Sinervo,³² A. Sisakyan,¹³ J. Sjolin,⁴¹ A. Skiba,²⁵ A. J. Slaughter,¹⁵ K. Sliwa,⁵⁵ D. Smirnov,³⁶ J. R. Smith,⁶ F. D. Snider,¹⁵ R. Snihur,³² M. Soderberg,³³ A. Soha,⁶ S. V. Somalwar,⁵⁰ J. Spalding,¹⁵ M. Spezziga,⁵² F. Spinella,⁴⁴ P. Squillacioti,⁴⁴ H. Stadie,²⁵ M. Stanitzki,⁵⁹ B. Stelzer,³² O. Stelzer-Chilton,³² D. Stentz,³⁷ J. Strologas,³⁶ D. Stuart,⁹ J. S. Suh,²⁷ A. Sukhanov,¹⁶ K. Sumorok,³¹ H. Sun,⁵⁵ T. Suzuki,⁵⁴ A. Taffard,²³ R. Tafirout,³² H. Takano,⁵⁴ R. Takashima,²² Y. Takeuchi,⁵⁴ K. Takikawa,⁵⁴ M. Tanaka,² R. Tanaka,³⁹ N. Tanimoto,³⁹ M. Tecchio,³³ P. K. Teng,¹ K. Terashi,⁴⁸ R. J. Tesarek,¹⁵ S. Tether,³¹ J. Thom,¹⁵ A. S. Thompson,¹⁹ E. Thomson,⁴³ P. Tipton,⁴⁷ V. Tiwari,¹¹ S. Tkaczyk,¹⁵ D. Toback,⁵¹ K. Tollefson,³⁴ T. Tomura,⁵⁴ D. Tonelli,⁴⁴ M. Tönnemann,³⁴ S. Torre,⁴⁴ D. Torretta,¹⁵ S. Tourneur,¹⁵ W. Trischuk,³² R. Tsuchiya,⁵⁶ S. Tsuno,³⁹ D. Tsybychev,¹⁶ N. Turini,⁴⁴ F. Ukegawa,⁵⁴ T. Unverhau,¹⁹ S. Uozumi,⁵⁴ D. Usynin,⁴³ L. Vacavant,²⁸ A. Vaiciulis,⁴⁷ A. Varganov,³³ S. Vejck III,¹⁵ G. Velez,¹⁵ V. Veszpremi,⁴⁶ G. Veramendi,²³ T. Vickey,²³ R. Vidal,¹⁵ I. Vila,¹⁰ R. Vilar,¹⁰ I. Vollrath,³² I. Volobouev,²⁸ M. von der Mey,⁷ P. Wagner,⁵¹ R. G. Wagner,² R. L. Wagner,¹⁵ W. Wagner,²⁵ R. Wallny,⁷ T. Walter,²⁵ Z. Wan,⁵⁰ M. J. Wang,¹ S. M. Wang,¹⁶ A. Warburton,³² B. Ward,¹⁹ S. Waschke,¹⁹ D. Waters,³⁰ T. Watts,⁵⁰ M. Weber,²⁸ W. C. Wester III,¹⁵ B. Whitehouse,⁵⁵ D. Whiteson,⁴³ A. B. Wicklund,² E. Wicklund,¹⁵ H. H. Williams,⁴³ P. Wilson,¹⁵ B. L. Winer,³⁸ P. Wittich,⁴³ S. Wolbers,¹⁵ C. Wolfe,¹² M. Wolter,⁵⁵ M. Worcester,⁷ S. Worm,⁵⁰ T. Wright,³³ X. Wu,¹⁸ F. Würthwein,⁸ A. Wyatt,³⁰ A. Yagil,¹⁵ K. Yamamoto,⁴⁰ T. Yamashita,³⁹ J. Yamaoka,⁵⁰ C. Yang,⁵⁹ U. K. Yang,¹² W. Yao,²⁸ G. P. Yeh,¹⁵ J. Yoh,¹⁵ K. Yorita,⁵⁶ T. Yoshida,⁴⁰ I. Yu,²⁷ S. Yu,⁴³ J. C. Yun,¹⁵ L. Zanello,⁴⁹ A. Zanetti,⁵³ I. Zaw,²⁰ F. Zetti,⁴⁴ J. Zhou,⁵⁰ and S. Zucchelli⁴

(CDF Collaboration)

¹*Institute of Physics, Academia Sinica, Taipei, Taiwan 11529, Republic of China*²*Argonne National Laboratory, Argonne, Illinois 60439, USA*³*Institut de Física d'Altes Energies, Universitat Autònoma de Barcelona, E-08193, Bellaterra (Barcelona), Spain*⁴*Istituto Nazionale di Fisica Nucleare, University of Bologna, I-40127 Bologna, Italy*⁵*Brandeis University, Waltham, Massachusetts 02254, USA*⁶*University of California at Davis, Davis, California 95616, USA*⁷*University of California at Los Angeles, Los Angeles, California 90024, USA*⁸*University of California at San Diego, La Jolla, California 92093, USA*⁹*University of California at Santa Barbara, Santa Barbara, California 93106, USA*¹⁰*Instituto de Física de Cantabria, CSIC-University of Cantabria, 39005 Santander, Spain*¹¹*Carnegie Mellon University, Pittsburgh, Pennsylvania 15213, USA*¹²*Enrico Fermi Institute, University of Chicago, Chicago, Illinois 60637, USA*¹³*Joint Institute for Nuclear Research, RU-141980 Dubna, Russia*¹⁴*Duke University, Durham, North Carolina 27708*¹⁵*Fermi National Accelerator Laboratory, Batavia, Illinois 60510, USA*¹⁶*University of Florida, Gainesville, Florida 32611, USA*¹⁷*Laboratori Nazionali di Frascati, Istituto Nazionale di Fisica Nucleare, I-00044 Frascati, Italy*¹⁸*University of Geneva, CH-1211 Geneva 4, Switzerland*¹⁹*Glasgow University, Glasgow G12 8QQ, United Kingdom*²⁰*Harvard University, Cambridge, Massachusetts 02138, USA*²¹*Division of High Energy Physics, Department of Physics, University of Helsinki and Helsinki Institute of Physics, FIN-00014, Helsinki, Finland*²²*Hiroshima University, Higashi-Hiroshima 724, Japan*²³*University of Illinois, Urbana, Illinois 61801, USA*²⁴*The Johns Hopkins University, Baltimore, Maryland 21218, USA*

- ²⁵*Institut für Experimentelle Kernphysik, Universität Karlsruhe, 76128 Karlsruhe, Germany*
²⁶*High Energy Accelerator Research Organization (KEK), Tsukuba, Ibaraki 305, Japan*
²⁷*Center for High Energy Physics, Kyungpook National University, Taegu 702-701; Seoul National University, Seoul 151-742; and SungKyunKwan University, Suwon 440-746, Korea*
²⁸*Ernest Orlando Lawrence Berkeley National Laboratory, Berkeley, California 94720, USA*
²⁹*University of Liverpool, Liverpool L69 7ZE, United Kingdom*
³⁰*University College London, London WC1E 6BT, United Kingdom*
³¹*Massachusetts Institute of Technology, Cambridge, Massachusetts 02139, USA*
³²*Institute of Particle Physics, McGill University, Montréal, Canada H3A 2T8; and University of Toronto, Toronto, Canada M5S 1A7*
³³*University of Michigan, Ann Arbor, Michigan 48109, USA*
³⁴*Michigan State University, East Lansing, Michigan 48824, USA*
³⁵*Institution for Theoretical and Experimental Physics, ITEP, Moscow 117259, Russia*
³⁶*University of New Mexico, Albuquerque, New Mexico 87131, USA*
³⁷*Northwestern University, Evanston, Illinois 60208, USA*
³⁸*The Ohio State University, Columbus, Ohio 43210, USA*
³⁹*Okayama University, Okayama 700-8530, Japan*
⁴⁰*Osaka City University, Osaka 588, Japan*
⁴¹*University of Oxford, Oxford OX1 3RH, United Kingdom*
⁴²*University of Padova, Istituto Nazionale di Fisica Nucleare, Sezione di Padova-Trento, I-35131 Padova, Italy*
⁴³*University of Pennsylvania, Philadelphia, Pennsylvania 19104, USA*
⁴⁴*Istituto Nazionale di Fisica Nucleare, University and Scuola Normale Superiore of Pisa, I-56100 Pisa, Italy*
⁴⁵*University of Pittsburgh, Pittsburgh, Pennsylvania 15260, USA*
⁴⁶*Purdue University, West Lafayette, Indiana 47907, USA*
⁴⁷*University of Rochester, Rochester, New York 14627, USA*
⁴⁸*The Rockefeller University, New York, New York 10021, USA*
⁴⁹*Istituto Nazionale di Fisica Nucleare, Sezione di Roma 1, University di Roma "La Sapienza," I-00185 Roma, Italy*
⁵⁰*Rutgers University, Piscataway, New Jersey 08855, USA*
⁵¹*Texas A&M University, College Station, Texas 77843, USA*
⁵²*Texas Tech University, Lubbock, Texas 79409, USA*
⁵³*Istituto Nazionale di Fisica Nucleare, University of Trieste, Udine, Italy*
⁵⁴*University of Tsukuba, Tsukuba, Ibaraki 305, Japan*
⁵⁵*Tufts University, Medford, Massachusetts 02155, USA*
⁵⁶*Waseda University, Tokyo 169, Japan*
⁵⁷*Wayne State University, Detroit, Michigan 48201, USA*
⁵⁸*University of Wisconsin, Madison, Wisconsin 53706, USA*
⁵⁹*Yale University, New Haven, Connecticut 06520, USA*

(Received 25 October 2004; published 2 June 2005; corrected 10 June 2005)

We report on a search for the pair production of scalar leptoquarks (LQ), using 191 pb^{-1} of proton-antiproton collision data recorded by the CDF experiment during Run II of the Tevatron. The leptoquarks are sought via their decay into a neutrino and quark yielding missing transverse energy and several jets of large transverse energy. No evidence for LQ production is observed, and limits are set on $\sigma(p\bar{p} \rightarrow \text{LQL}\bar{Q}X \rightarrow \nu\bar{\nu}q\bar{q}X)$. Using a next-to-leading order theoretical prediction of the cross section for LQ production, we exclude first-generation LQ in the mass interval 78 to 117 GeV/c^2 at the 95% confidence level for $BR(\text{LQ} \rightarrow \nu q) = 100\%$.

DOI: 10.1103/PhysRevD.71.112001

PACS numbers: 13.85.Rm, 12.60.-i, 14.80.-j

The remarkable symmetry between quarks and leptons in the standard model (SM) suggests that some more fundamental theory may exist, which allows interactions between them. Such interactions may be mediated by a new type of particle, a leptoquark [1], which carries both lepton and baryon number. A leptoquark is a color-triplet boson with spin 0 or 1, and has fractional electric charge. Leptoquarks are predicted in many extensions of the SM (e.g. grand unification, technicolor, and supersymmetry with R -parity violation). The Yukawa coupling of the

leptoquark to a lepton and quark and the inclusive branching ratio to a charged lepton and quark, denoted by β , are model dependent. Usually it is assumed that leptoquarks couple to only one generation to accommodate experimental constraints on flavor-changing neutral currents [2], which allows one to classify leptoquarks as first-, second-, or third-generation, with decay products corresponding to the three generations of fermions in SM. In $p\bar{p}$ collisions, leptoquarks can be produced in pairs via the strong interaction through gg fusion or $q\bar{q}$ annihilation. The produc-

tion rate for scalar leptoquarks is essentially model-independent and is determined by the known QCD couplings and leptoquark mass. On the other hand, vector leptoquark interactions with the gluon field include model-dependent couplings. The production cross section for vector leptoquarks [3] is expected to be about an order of magnitude larger than that for scalar leptoquarks.

We report on a search for pair production of scalar leptoquarks, with LQ decaying to νq , resulting in a jets and missing transverse energy (\cancel{E}_T) topology. We use $191 \pm 11 \text{ pb}^{-1}$ [4] of $p\bar{p}$ collision data at a center-of-mass energy of 1.96 TeV recorded by the collider detector at Fermilab (CDF) during the Tevatron Run II. This analysis is sensitive to leptoquarks of all three generations with $\beta \approx 0$. However, we would not be able to distinguish between the different generations of leptoquarks, if they are present in the signal, since we do not identify the quark content of the jets. The previous lower mass limit of $98 \text{ GeV}/c^2$ [5] on first-generation leptoquarks in this final state was set by the DØ Collaboration. The CDF Collaboration has also published [6] lower mass limits of $123 \text{ GeV}/c^2$ and $148 \text{ GeV}/c^2$ respectively on second- and third-generation LQ in the \cancel{E}_T plus heavy-flavor jets final state. Limits on leptoquark production from the Tevatron Run I and HERA experiments as of 1999 are summarized in [7]. The limits from HERA experiments depend on the unknown Yukawa couplings, which are assumed to be of the electro-weak coupling strength. The OPAL collaboration published [8] mass limits of $97 \text{ GeV}/c^2$ independent of the Yukawa couplings for the scalar LQ production into $\nu\bar{\nu}q\bar{q}$ final state in e^+e^- -collision.

CDF is a general-purpose detector that is described in detail elsewhere [9]. The components relevant to this analysis are briefly described here. The charged-particle tracking system is closest to the beam pipe, and consists of multilayer silicon detectors and a large open-cell drift chamber covering the pseudorapidity [10] region $|\eta| < 1$. The tracking system is enclosed in a superconducting solenoid, which in turn is surrounded by a calorimeter. The CDF calorimeter system is organized into electromagnetic and hadronic sections segmented in projective tower geometry, and covers the region $|\eta| < 3.6$. The electromagnetic calorimeters utilize a lead-scintillator sampling technique, whereas the hadron calorimeters use iron-scintillator technology. The central muon-detection system, used for this analysis, is located outside of the calorimeter and covers the range $|\eta| < 1$.

This search centers on selecting events with large \cancel{E}_T and a pair of jets that are acollinear in the transverse plane, because of the neutrinos in the final state. The \cancel{E}_T [10] is defined as the energy imbalance in the plane transverse to the beam direction. A jet is defined as a localized energy deposition in the calorimeter and is reconstructed using a cone algorithm with fixed radius $\Delta R \equiv \sqrt{\Delta\eta^2 + \Delta\phi^2} = 0.4$ in $\eta - \phi$ space [11]. We correct [11] jet E_T measurements and \cancel{E}_T for detector effects.

The data sample for this analysis was collected using an inclusive \cancel{E}_T trigger, which is distributed across three levels of online event selection. In the first and second levels of the trigger, \cancel{E}_T is required to be greater than 25 GeV and is calculated by summing over calorimeter trigger towers [12] with transverse energies above 1 GeV. At Level-3 \cancel{E}_T is required to be greater than 45 GeV and is recalculated using full calorimeter segmentation with a tower energy threshold of 100 MeV. We use events from the inclusive high- p_T lepton (e or μ) samples to measure the trigger efficiency directly from data. To reduce systematic effects associated with the online trigger threshold, we select events offline with $\cancel{E}_T > 60 \text{ GeV}$, where the trigger is fully efficient.

The event electromagnetic fraction (F_{em}) and charged fraction (F_{ch}) [13] are used to remove events associated with beam halo and cosmic ray sources. We reject events that contain little energy in the electromagnetic section of the calorimeter or that have mostly neutral-particle jets, by requiring $F_{\text{em}} > 0.1$ and $F_{\text{ch}} > 0.1$. There are 148 462 events in our analysis sample after the initial selection.

The dominant backgrounds to the leptoquark search in the jets and \cancel{E}_T signature are QCD multijet production, W and Z boson production in association with one or more jets, and top quark pair production. The ALPGEN generator [14] was used for the simulation of the W and Z boson plus parton production, with HERWIG [15] used to model parton showers. As the W/Z + jets production cross sections calculated by ALPGEN are only in leading order, we use the exclusive $Z(\rightarrow ee) + 1$ jet data and simulation samples to determine a cross section scale-factor between data and simulation, and apply this scale-factor to all W/Z + jets simulation samples. HERWIG was also used to estimate the contribution from $t\bar{t}$ production. The top quark contribution was normalized to the luminosity of the data sample using the predicted theoretical cross section.

Data selection requirements were chosen to maximize the statistical significance of the leptoquark signal over background events based on studies of simulated event samples before the signal region data were examined. In addition to $\cancel{E}_T > 60 \text{ GeV}$, the signal region is defined by requiring that the two highest E_T jets ($E_T^{j_1} > 40 \text{ GeV}$, $E_T^{j_2} > 25 \text{ GeV}$) be in the central region $|\eta| < 1$. A third jet with $E_T > 15 \text{ GeV}$ and $|\eta| < 2.5$ is allowed, and we veto events with any additional jets with $E_T > 15 \text{ GeV}$ and $|\eta| < 3.6$. To reject events with \cancel{E}_T resulting from jet energy mismeasurement, we require that the opening angle in the transverse plane between the two highest E_T jets satisfy $80^\circ < \Delta\phi(j_1, j_2) < 165^\circ$. The \cancel{E}_T direction must not be parallel to any of the jets; we require the minimum azimuthal separation between the direction of the jets and \cancel{E}_T to satisfy $30^\circ < \min\Delta\phi(j, \cancel{E}_T) < 135^\circ$. The \cancel{E}_T also must not be antiparallel to the leading E_T jet: $100^\circ < \Delta\phi(j_1, \cancel{E}_T) < 165^\circ$. These criteria reject most of the QCD multijet background events. To reduce the back-

ground contribution from $W/Z + \text{jets}$ and $t\bar{t}$ production, we reject events with one or more identified leptons with $E_T > 10$ GeV (electron candidates) or $p_T > 10$ GeV/ c (muon candidates). Criteria similar to those in [16] are used to identify the leptons. To further reduce this background we require each jet not to be highly electromagnetic (jet electromagnetic fraction < 0.9) and to have 4 or more associated tracks for central jets ($|\eta| < 1$).

Two methods are employed to estimate the QCD multi-jet contribution in the signal region directly from the inclusive \cancel{E}_T data sample. Among all the offline analysis selection requirements, the azimuthal angular separation requirement between the \cancel{E}_T direction and a jet is most effective at removing QCD multijet events. Therefore, for the first method, in addition to the signal region we define a region which is rich in QCD multijet events by requiring that a jet is close to the \cancel{E}_T direction ($20^\circ < \min\Delta\phi(j, \cancel{E}_T) < 27^\circ$). Studies of simulated QCD multijet samples show that the shape of the \cancel{E}_T distribution in this region is similar to the \cancel{E}_T distribution in the signal region. We use \cancel{E}_T and $\min\Delta\phi(j, \cancel{E}_T)$ requirements to define four kinematic regions:

- (A) $50 < \cancel{E}_T < 57$ GeV, $20^\circ < \min\Delta\phi(j, \cancel{E}_T) < 27^\circ$.
- (B) $\cancel{E}_T > 60$ GeV, $20^\circ < \min\Delta\phi(j, \cancel{E}_T) < 27^\circ$.
- (C) $50 < \cancel{E}_T < 57$ GeV, $30^\circ < \min\Delta\phi(j, \cancel{E}_T) < 135^\circ$.
- (D) $\cancel{E}_T > 60$ GeV, $30^\circ < \min\Delta\phi(j, \cancel{E}_T) < 135^\circ$.

The regions A, B, and C are used to extrapolate the QCD multijet contribution into the signal region D : $N_D = \frac{N_B}{N_A} N_C$, where N_A , N_B , and N_C are the remaining number of events in regions A, B, and C, after the $W/Z + \text{jets}$ and $t\bar{t}$ contributions have been subtracted. For the second method, the combined selection requirement efficiency is measured as a function of \cancel{E}_T in an independent inclusive jet sample at low \cancel{E}_T . The extrapolated results of this measurement is then applied to the inclusive \cancel{E}_T sample after the $W/Z + \text{jets}$ and $t\bar{t}$ contributions have been subtracted. We predict 15.0 ± 8.0 and 21.5 ± 12.4 multijet events for the first and second methods, respectively. We take the weighted average and uncertainty of the two methods as our estimate of the multijet background.

We check the simulation predictions for $W/Z + \text{jets}$ with data in a control region, which is defined by requiring, in addition to 2 or 3 jets, $\cancel{E}_T > 60$ GeV and at least one electron or muon. We observe 144 events in our inclusive \cancel{E}_T sample, which is in excellent agreement with 154.3 ± 27.9 events predicted from SM processes.

The total detection efficiency (ϵ_{LQ}) for the scalar leptoquark signal is estimated using the PYTHIA event generator [17], and the CDF detector simulation program. The PYTHIA underlying event simulation was tuned to reproduce CDF data [18]. The samples were generated using the CTEQ5L [19] parton distribution functions (PDF), with the renormalization and factorization scales set to $\mu = m_{\text{LQ}}$. Table I lists the total detection efficiency, ϵ_{LQ} , for the first-generation scalar leptoquark signal and the corresponding

TABLE I. Summary of the first-generation scalar leptoquark detection efficiency (ϵ_{LQ}), the relative uncertainty on detection efficiency (δ_{tot}), and the next-to-leading order cross section (σ_{NLO}) for two choices of the renormalization scale as functions of leptoquark mass.

m_{LQ_1} (GeV/ c^2)	ϵ_{LQ_1}	δ_{tot} (%)	σ_{NLO} (pb)	
			$\mu = m_{\text{LQ}_1}$	$\mu = 2m_{\text{LQ}_1}$
75	0.0073	29	69.4	58.8
80	0.0113	26	49.2	41.5
90	0.0187	23	26.0	22.1
100	0.0300	20	14.6	12.5
110	0.0431	16	8.4	7.4
115	0.0482	15	6.7	5.8
125	0.0590	15	4.2	3.6
150	0.0828	13	1.4	1.3
175	0.1010	12	0.57	0.51

total fractional uncertainty δ_{tot} for various leptoquark masses. The acceptances for second- and third-generation leptoquark signals are estimated to be 4% and 10% lower, respectively, than that for the first generation in the generated mass region due to semileptonic decays of heavy-flavor quarks. Also listed are the NLO cross sections [20] calculated for two choices of the μ scale. The systematic uncertainty on the signal acceptance includes the uncertainties due to modeling gluon radiation from the initial-state or final-state partons (10%), and the choice of the PDF (4%). The limited size of the leptoquark simulation samples gives a 3% statistical uncertainty. The signal acceptance uncertainty due to the jet energy scale varies from 4% to 26%, and the uncertainty on the luminosity is 6%. The uncertainty on the trigger efficiency is 1%. The theoretical uncertainties on the renormalization and factorization scales are not included here, since we conservatively choose the NLO cross section setting $\mu = 2m_{\text{LQ}}$ to extract the limits on leptoquark mass. This choice of scale is found to reduce the cross section prediction by 15% relative to $\mu = m_{\text{LQ}}$ [20].

TABLE II. The number of expected events from various SM sources in the leptoquark signal region. The first uncertainty is from the limited simulation statistics and the second is from the various systematics.

Source	Events expected
$W(\rightarrow e\nu) + \text{jets}$	$6.1 \pm 1.4 \pm 1.5$
$W(\rightarrow \mu\nu) + \text{jets}$	$21.7 \pm 2.3 \pm 2.8$
$W(\rightarrow \tau\nu) + \text{jets}$	$28.4 \pm 3.8 \pm 4.1$
$Z(\rightarrow \mu\mu) + \text{jets}$	$1.1 \pm 0.2 \pm 0.2$
$Z(\rightarrow \tau\tau) + \text{jets}$	$0.9 \pm 0.2 \pm 0.2$
$Z(\rightarrow \nu\nu) + \text{jets}$	$39.1 \pm 2.8 \pm 3.6$
$t\bar{t}$	$4.3 \pm 0.4 \pm 0.3$
QCD	16.9 ± 6.7
Total events	118.5 ± 14.5

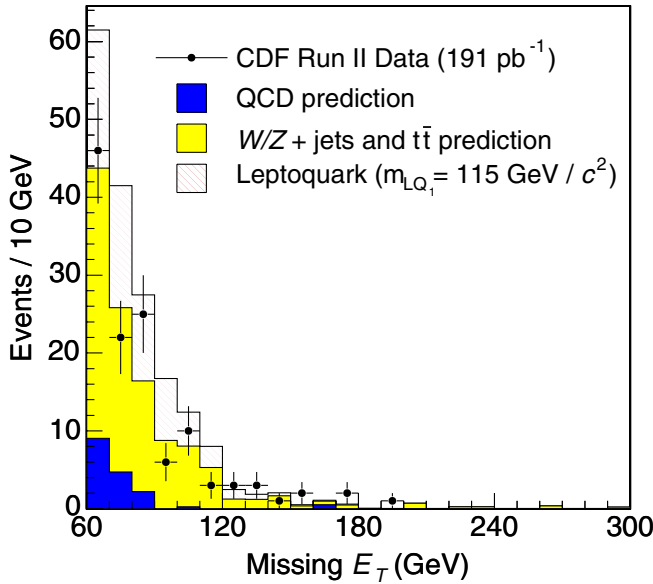


FIG. 1 (color online). The \cancel{E}_T distribution in the leptoquark signal region for data (solid points) compared to SM background (shaded histograms). Also shown is the expected distribution arising from leptoquark production and decay at a mass of $115 \text{ GeV}/c^2$ (hatched histogram).

In the signal region, we expect 118.5 ± 14.5 events from SM processes and observe 124 events. The predicted backgrounds from SM processes are summarized in Table II. In Fig. 1 the predicted \cancel{E}_T distribution is compared with the distribution observed in data. No evidence for leptoquark production is observed. We calculate the upper limit at the 95% confidence level (C.L.) on the pair production cross section times the square of the branching ratio of the leptoquark to a quark and a neutrino using first-generation LQ acceptance and a Bayesian approach [21] with a flat prior for the signal cross section and Gaussian priors for acceptance and background uncertainties. The upper limit on the cross section times $(1 - \beta)^2$ is shown in Fig. 2 and is compared with the theoretical cross sections. The theoretical cross sections for scalar leptoquark production have been calculated at NLO using CTEQ5M [19] PDFs.

In conclusion, we performed a search for leptoquarks in the jets and \cancel{E}_T topology using 191 pb^{-1} of CDF Run II data. No evidence for leptoquarks is observed. We set an upper limit on the production cross section at the 95% C.L. Assuming a leptoquark decays into a neutrino and quark with 100% branching ratio, we exclude the mass interval from 78 to $117 \text{ GeV}/c^2$ for first-generation LQ independent of the Yukawa coupling. This extends the previous

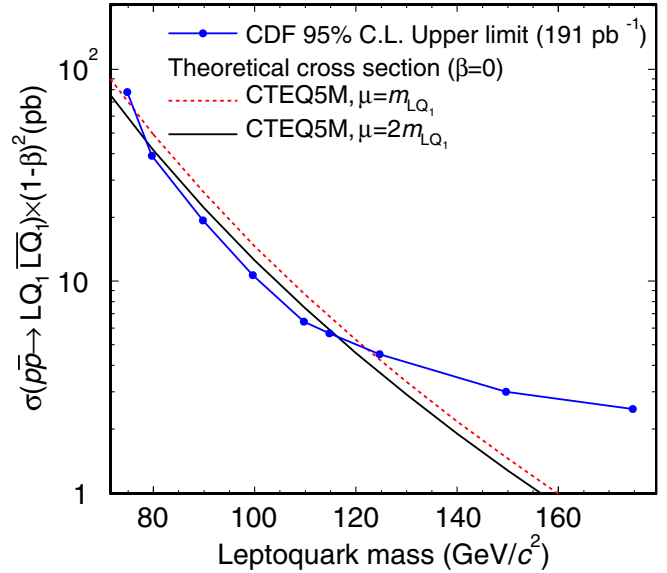


FIG. 2 (color online). The upper limit on the cross section times squared branching ratio for scalar leptoquark production in the jets and \cancel{E}_T topology. Also shown is the NLO cross section for $\beta = 0$ for 2 choices of the factorization/renormalization scale: $\mu = m_{LQ_1}$, $\mu = 2m_{LQ_1}$.

limit for the first-generation LQ of $98 \text{ GeV}/c^2$ [5]. The limits for the second- and third-generation LQ are weaker than existing limits obtained from an exclusive search [6] identifying jet flavor.

We thank the Fermilab staff and the technical staffs of the participating institutions for their vital contributions. This work was supported by the U.S. Department of Energy and National Science Foundation; the Italian Istituto Nazionale di Fisica Nucleare; the Ministry of Education, Culture, Sports, Science and Technology of Japan; the Natural Sciences and Engineering Research Council of Canada; the National Science Council of the Republic of China; the Swiss National Science Foundation; the A. P. Sloan Foundation; the Bundesministerium fuer Bildung und Forschung, Germany; the Korean Science and Engineering Foundation and the Korean Research Foundation; the Particle Physics and Astronomy Research Council and the Royal Society, U.K.; the Russian Foundation for Basic Research; the Comision Interministerial de Ciencia y Tecnologia, Spain; in part by the European Community's Human Potential Programme under Contract No. HPRN-CT-2002-00292; and the Academy of Finland.

- [1] W. Buchmüller, R. Rückl, and D. Wyler, Phys. Lett. B **191**, 442 (1987); **448**, 320E (1999).
- [2] S. Davidson, D. Bailey, and B. A. Campbell, Z. Phys. C **61**, 613 (1994).
- [3] J. Blümlein, E. Boos, and A. Kryukov, Z. Phys. C **76**, 137 (1997).
- [4] S. Klimenko, J. Konigsberg, and T. Liss, Report No. FERMILAB-FN-0741, 2003; D. Acosta *et al.*, Nucl. Instrum. Methods Phys. Res., Sect. A **494**, 57 (2002).
- [5] V. M. Abazov *et al.*, Phys. Rev. Lett. **88**, 191801 (2002).
- [6] T. Affolder *et al.* (CDF Collaboration), Phys. Rev. Lett. **85**, 2056 (2000).
- [7] D. E. Acosta and S. K. Blessing, Annu. Rev. Nucl. Part. Sci. **49**, 389 (1999).
- [8] G. Abbiendi *et al.* (OPAL Collaboration), Eur. Phys. J. C **31**, 281 (2003).
- [9] R. Blair *et al.* CDF Collaboration, Report No. FERMILAB-PUB-96/390-E.
- [10] CDF uses a cylindrical coordinate system in which θ is the polar angle to the proton beam, ϕ is the azimuthal angle about the beam axis, and pseudorapidity is defined as $\eta = -\text{Intan}(\theta/2)$. The transverse energy and transverse momentum are defined as $E_T = E \sin\theta$ and $p_T = p \sin\theta$, where E is energy measured in the calorimeter and p is momentum measured by the tracking system. The missing transverse energy vector, \vec{E}_T , is $-\sum_i E_T^i \mathbf{n}_i$, where \mathbf{n}_i is the unit vector in the azimuthal plane that points from the beamline to the i th calorimeter tower.
- [11] F. Abe *et al.* (CDF Collaboration), Phys. Rev. D **45**, 1448 (1992).
- [12] The physical calorimeter towers are organized into larger trigger towers, covering approximately 0.26 in $\Delta\phi$ and 0.22 in $\Delta\eta$.
- [13] F_{em} is the ratio of the energy measured by the electromagnetic calorimeter to the total energy contained in jets of cone radius $\Delta R = 0.4$ with $E_T > 10$ GeV and $|\eta| < 3.6$. F_{ch} is the fraction of the jet energy carried by measured charged-particle tracks ($p_T > 0.5$ GeV/ c) averaged over the central jets with $|\eta| < 0.9$. These variables are similar to ones used in T. Affolder *et al.* (CDF Collaboration), Phys. Rev. Lett. **88**, 041801 (2002).
- [14] M. L. Mangano *et al.*, J. High Energy Phys. 07 (2003) 001. We use version 1.2.
- [15] G. Corcella *et al.*, J. High Energy Phys. 01 (2001) 010; hep-ph/0210213. We use version 6.4a.
- [16] D. Acosta *et al.* (CDF Collaboration), Phys. Rev. Lett. **93**, 142001 (2004).
- [17] T. Sjostrand *et al.*, Comput. Phys. Commun. **135**, 238 (2001), version 6.203.
- [18] T. Affolder *et al.* (CDF Collaboration), Phys. Rev. D **65**, 092002 (2002).
- [19] H. L. Lai *et al.* (CTEQ Collaboration), Eur. Phys. J. C **12**, 375 (2000).
- [20] M. Krämer, T. Plehn, M. Spira, and P. M. Zerwas, Phys. Rev. Lett. **79**, 341 (1997).
- [21] J. Conway, CERN Report No. 2000-005, 2000, 247. The posterior probability density is rendered normalizable by introducing a reasonably large cutoff.